Spatial Restoration with Reduced Boundary Error

Jaehoon Koo and N. K. Bose
121 Electrical Engineering East
The Pennsylvania State University
University Park, PA 16802
USA

Abstract

Since any symmetric **BTHTHB** matrix can be diagonalized by the **DCT** matrix, a **BTTB** matrix encountered in the image reconstruction problem is sometimes approximated by a **BTHTHB** matrix for computational efficiency. In this paper, the error caused by the approximation of a **BTTB** matrix by a **BTHTHB** matrix is analyzed. It is also shown that a simple modification of the observed image can achieve both reduced boundary error and fast deblurring.

1 Introduction

Nowadays, we encounter digital color images more than monochrome images with the advent of digital TV and fast internet infrastructure. The global wide sense stationarity assumption is pervasive in several known methods spanning the work of Hunt and Kubler in 1984 upto the work of Boo and Bose in 1997 for multispectral images [1]. With the assumption that the estimates of signal power spectrum and noise power spectrum are available, a 3-D Wiener filter was applied to two luminance images and 2-D Wiener filters to the chrominance components [1]. However, the approximation of **BTTB** (Block Toeplitz Toeplitz Block) by **BCCB** (Block Circulant Circulant Block) matrix caused some image degradation due to leakage components near the zeros of the transfer function characterizing the linear shift-invariant (**LSI**) blur [2]. The amplified leakage component may cause ringing effect near boundaries as well as in the center part of image. In [2], the observed image is extrapolated and the image reconstruction is performed in **DFT** domain with the periodic boundary condition to reduce this effect. In [3], the blur matrix was modified so that the blur function has more peaked distribution near the boundaries. However, this modification destroys the **BCCB** structure , so that diagonalization by 2-D **DFT** is not possible. The Neumann boundary condition is known to produce small boundary error if the image is stationary inside and as well as outside the boundaries [4]. Also, the resulting **BTHTHB** (Block Toeplitz-plus-Hankel Toeplitz-plus-Hankel Block) matrix from the Neumann boundary condition can be diagonalized by the **DCT** matrix if the **BTHTHB** matrix is symmetric [4].

The approximation of **BTTB** by **BTHTHB**, however, also produces unwanted ringing effects similar to that in the approximation of **BTTB** by **BCCB**. Here, it will be shown that simple modification of the observed image can significantly reduce the ringing effect while keeping the **BTHTHB** structure invariant. With the technique introduced here, it is possible to achieve both fast deblurring and reduced boundary error.

2 Main Results

For brevity, consider the 1-D case. Denote the original finite dimensional signal vector by

$$\mathbf{f} = (..., f_{-m+1}, ..., f_o, f_1, ...f_n, f_{n+1}, ..., f_{n+m}, ...)^t$$

and the blur vector by

$$\mathbf{h} = (..., 0, h_{-m}, ..., h_0, ...h_m, 0, ...)^t. \tag{1}$$

The convolution $\mathbf{h}^t * \mathbf{f}^t$ produces the blurred signal vector $\mathbf{g} = [g_1, ..., g_n]^t$, where [4]

$$\mathbf{T}_l\mathbf{f}_l + \mathbf{T}\mathbf{f} + \mathbf{T}_r\mathbf{f}_r = \mathbf{g}, \tag{2}$$

$$\mathbf{f}_l = [f_{-m+1}, f_{-m+2}, ..., f_{-1}, f_0]^t, \quad \mathbf{f} = [f_1, f_2, ..., f_{n-1}, f_n]^t, \quad \mathbf{f}_r = [f_{n+1}, f_{n+2}, ..., f_{n+m-1}, f_{n+m}]^t,$$

$$\mathbf{T}_l = \begin{bmatrix} h_m & \cdots & h_1 \\ & \ddots & \ddots \\ & & h_m \\ 0 & & \end{bmatrix}, \quad \mathbf{T} = \begin{bmatrix} h_0 & \cdots & h_{-m} & & \\ \vdots & \ddots & \ddots & \ddots & \\ h_m & \ddots & \ddots & \ddots & h_{-m} \\ & \ddots & \ddots & \ddots & \vdots \\ & & h_m & \cdots & h_0 \end{bmatrix}, \quad \mathbf{T}_r = \begin{bmatrix} & & 0 \\ & & \\ h_{-m} & & \\ \vdots & \ddots & \\ h_{-1} & \cdots & h_{-m} \end{bmatrix}.$$

In the case of Neumann boundary condition, the data outside the support of $\mathbf{f}$ is assumed to be a reflection of the data inside the support of $\mathbf{f}$, i.e.,

$$f_j = f_k, \quad \text{where} \begin{cases} k = 1 - j, & \text{if} \quad i < 1 \\ k = 2n + 1 - i, & \text{if} \quad i > n \end{cases}$$

Then the system of equations in Eq. (2) becomes [4] (J denotes the anti-identity matrix satisfying $J^2 = I$ and $\mathbf{H}^{(n)} = [(0|\mathbf{T}_l)J + \mathbf{T} + (\mathbf{T}_r|0)J]$)

$$\mathbf{g} = [(0|\mathbf{T}_l)J + \mathbf{T} + (\mathbf{T}_r|0)J]\mathbf{f} = \mathbf{H}^{(n)}\mathbf{f}. \tag{3}$$

The resulting blur matrix $\mathbf{H}^{(n)}$ is a Toeplitz-plus-Hankel matrix, which can be diagonalized by a **DCT** matrix *if it is symmetric* [4]. In the 2-D case, the blur matrix becomes a **BTHTHB** matrix, which can be diagonalized by the 2-D **DCT** matrix.

The image reconstruction system described in Eq. (2) is known to be ill-posed. The Tikhonov regularized solution minimizes the objective function,

$$\min_{\mathbf{f}} \ ||\mathbf{H}\mathbf{f} - \mathbf{g}||_2^2 + \lambda||\mathbf{L}\mathbf{f}||_2^2 \tag{4}$$

where $\mathbf{L}$ is the smoothing Laplacian-like operator and λ is the regularization parameter, optimally calculable may be calculated by the L-curve [5] or other methods. It is easy to show that the solution of Eq. (4) is

$$\mathbf{f}_\lambda = \left[\mathbf{H}^t\mathbf{H} + \lambda\mathbf{L}^t\mathbf{L}\right]^{-1}\mathbf{H}^t\mathbf{g}.$$

Space-variant regularization methods have also been proposed [6].

Theorem 1 *[4] With $\lambda > 0$, let $\mathbf{f}_\lambda^{(n)}$ be the regularized solution with the Neumann boundary condition. Then the error vector $\mathbf{e}_\lambda^{(n)} \equiv \mathbf{f}_\lambda^{(n)} - \mathbf{f}$ of the reconstructed signal can be decomposed as the sum $\mathbf{e}_\lambda^{(n)R} + \mathbf{e}_\lambda^{(n)B}$ of the regularization error $\mathbf{e}_\lambda^{(n)R}$ and boundary error $\mathbf{e}_\lambda^{(n)B}$. The boundary error, $\mathbf{e}_\lambda^{(n)B}$ can be expressed as*

$$\mathbf{e}_\lambda^{(n)B} = [\mathbf{H}^{(n)t}\mathbf{H}^{(n)} + \lambda \mathbf{L}^t\mathbf{L}]^{-1}\mathbf{H}^{(n)t}\{[\mathbf{T}_l\mathbf{f}_l - (0|\mathbf{T}_l)J\mathbf{f}] + [\mathbf{T}_r\mathbf{f}_r - (\mathbf{T}_r|0)J\mathbf{f}]\}$$

Furthermore, if ($E(\mathbf{v})$ denotes the expected value of a random vector $\mathbf{v}$)

$$E([\mathbf{f}]_i) = \gamma_1, \quad -m+1 \le i \le m, \quad \textit{and} \quad E([\mathbf{f}]_i) = \gamma_2, \quad n-m+1 \le i \le n+m,$$

then

$$|E([\mathbf{e}_\lambda^{(n)B}]_i)| = 0$$

A method to satisfy the last equality with more relaxed constraints is proposed next. Rewrite Eq. (2) as

$$\begin{aligned}\mathbf{g} &= \mathbf{T}_l\mathbf{f}_l + \mathbf{T}\mathbf{f} + \mathbf{T}_r\mathbf{f}_r \\ &= [(0|\mathbf{T}_l)J + \mathbf{T} + (\mathbf{T}_r|0)J]\mathbf{f} + \mathbf{T}_l\mathbf{f}_l + \mathbf{T}_r\mathbf{f}_r - (0|\mathbf{T}_l)J\mathbf{f} - (\mathbf{T}_r|0)J\mathbf{f} \\ &= \mathbf{H}^{(n)}\mathbf{f} + \underbrace{[\mathbf{T}_l\mathbf{f}_l + \mathbf{T}_r\mathbf{f}_r - (0|\mathbf{T}_l)J\mathbf{f} - (\mathbf{T}_r|0)J\mathbf{f}]}_{BC\ error\ \mathbf{e}}\end{aligned} \tag{5}$$

where, $\mathbf{H}^{(n)}$ is a Toeplitz-plus-Hankel matrix, defined in Eq. (3)

The main contribution of this paper is summarized next.

Theorem 2 *If the original image is stationary near its boundary with conditions,*

$$E([\mathbf{f}]_i) = \gamma_1, \quad 1 \le i \le 3m, \quad \textit{and} \quad E([\mathbf{f}]_i) = \gamma_2, \quad n-3m+1 \le i \le n,$$

*for constants γ_1, γ_2, then with boundary condition (**BC**) error vector $\mathbf{e}$ defined in Eq. (5), the expected value of the random vector $\mathbf{e}$ is*

$$E(\mathbf{e}) = E([g_1 - g_{2m} \ \ g_2 - g_{2m-1} \ \ \cdots \ \ g_m - g_{m+1} \ \ 0 \ \ \cdots \ \ 0 \ \ g_{n-m+1} - g_{n-m} \ \ \cdots \ \ g_n - g_{n-2m+1}]^t)$$

Proof. ¿From Eq. (5), the k_{th} element e_k of vector $\mathbf{e}$ can be written as

$$e_k = \begin{cases} \sum_{t=k}^{m} h_t(f_{k-t} - f_{t-k+1}), & \text{for} \quad 1 \le k \le m \\ \sum_{t=-m}^{k-n-1} h_t(f_{k-t} - f_{2n+t+1-k}), & \text{for} \quad n-m+1 \le k \le n \\ 0, & \text{otherwise} \end{cases}$$

Then, for $1 \le k \le m$,

$$\begin{aligned} g_k - g_{2m-k+1} &= \sum_{t=-m}^{m} h_t(f_{-t+k} - f_{2m-t-k+1}) \\ &= \underbrace{\sum_{t=-m}^{k-1} h_t(f_{-t+k} - f_{2m-t-k+1})}_{term1} + \underbrace{\sum_{t=k}^{m} h_t(f_{t-k+1} - f_{2m-t-k+1})}_{term2} + e_k \end{aligned}$$

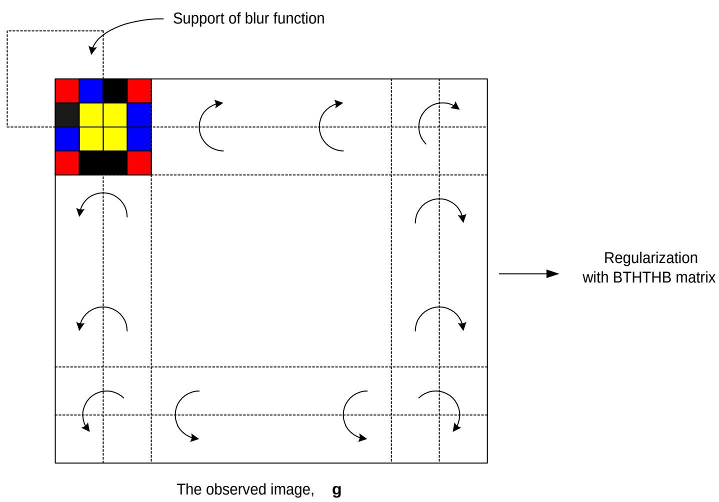

Figure 1: Modification of observed image $\mathbf{g}$

and for $n-m+1 \le k \le n$,

$$\begin{aligned} g_k - g_{2n-k-2m+1} &= \sum_{t=-m}^{m} h_t(f_{k-t} - f_{2n-k-2m-t+1}) \\ &= \underbrace{\sum_{t=k-n}^{m} h_t(f_{k-t} - f_{2n-k-2m-t+1})}_{term3} + \underbrace{\sum_{t=-m}^{k-n-1} h_t(f_{2n+t+1-k} - f_{2n-k-2m-t+1})}_{term4} + e_k. \end{aligned}$$

With the conditions stated above (**Theorem** 2) satisfied,

$$E(term1) = E(term2) = E(term3) = E(term4) = 0$$

Therefore, $E(\mathbf{e})$ has the form stated in the theorem. □

If the expected value of $\mathbf{g}$ is replaced by the instantaneous value of $\mathbf{g}$ in **Theorem** 2, then the observed image $\mathbf{g}$, after modification by the boundary error, is

$$\mathbf{g}_{mod} \triangleq \mathbf{g} - E(\mathbf{e}) \approx \mathbf{H}^{(n)}\mathbf{f} \tag{6}$$

(the $\approx$ sign becomes an equality when $E(\mathbf{e})$ is replaced by $\mathbf{e}$, as in the LMS algorithm [7]) where

$$\mathbf{g}_{mod} = [g_{2m}\ g_{2m-1}\ \cdots\ g_{m+1}\ g_{m+1}\ \cdots\ g_{n-m}\ g_{n-m}\ \cdots g_{n-2m+1}]^t \tag{7}$$

The k-th sample of the modified signal (with blur in Eq. 1) is

$$g_{mod\ k} = \begin{cases} g_{2m-k+1} & \text{for} \quad 1 \le k \le m \\ g_{2n-k-2m+1}, & \text{for} \quad n-m+1 \le k \le n \\ g_k, & \text{otherwise} \end{cases} \tag{8}$$

Therefore, before regularization is applied, the modifications in the observed signal occur in the first m elements as well as the last m elements (see Eq. 7).

In the case of 2-D signal, the modification shown in Eq. (8) is performed along horizontal and vertical directions, as described in Figure 1.

3 Computer Experiments

In this computer simulation, a 256×256 was taken to be the original image, as shown in Figure 2 (a). The observed image was generated by convolving the original image with a **LSI** uniform circular blur function of 6 pixels diameter and then adding a white Gaussian noise, as shown in Figure 2 (b). For comparison, two image reconstruction algorithms were performed: (1)**BTHTHB** approximation without the modification of the observed images (2)**BTHTHB** approximation with the modification suggested in this paper of the observed images. The reconstructed images by the two different methods are shown in Figures 2 (c) and (d). To get the optimal regularization parameter, the L-curve method [5] was used.

4 Conclusions

Without the modification of the observed image, the approximation of **BTTB** by **BTHTHB** causes ringing effect in the reconstructed image. However, simple modification of the observed image significantly reduces this effect, and leads to improvement of the visual image quality as well as PSNR (Peak Signal-to-Noise Ratio).

Acknowledgement: This research was supported in part by **ARO** Grant DAAD 19-00-1-0539.

References

[1] K. J. Boo and N. K. Bose, "Multispectral Image Restoration with Multisensors," *IEEE Transactions on Geoscience and Remote Sensing*, vol. 35, September 1997, pp. 1160-1170

[2] J. W. Woods, J. Biemond and A. M. Tekalp, "Boundary Value Problem in Image Restoration," *Proceedings, ICASSP*, March 1985, pp. 18.11.1-18.11.4

[3] F. T. Luk and D. Vandevoorde, "Reducing Boundary Distortion in Image Restoration," *Proceedings of SPIE, The International Society for Optical Engineering*, vol. 2296, July 1994, pp. 554-565.

[4] M. K. Ng and R. H. Chan and W. C. Tang, "A Fast Algorithm for Deblurring Models with Neumann Boundary Conditions, " *SIAM Journal of Scientific Computing*, vol. 21, no. 3, 1999, pp. 851-866.

[5] P. C. Hansen, "Analysis of Discrete Ill-Posed Problems by Means of the L-curve," *SIAM Review*, vol. 34, December 1992, pp. 561-580.

[6] S. J. Reeves, "Optimal Space-Varying Regularization in Iterative Image Restoration," *IEEE Transactions on Image Processing*, vol. 3, May 1994, pp. 319-324.

(a) Original image of size 256×256.

Observed blurred and noisy image; PSNR=24.53dB.

Restored image without data modification; PSNR=24.59dB.

Restored image with data modification; PSNR=27.09dB.

Figure 2: Image restoration with approximation of **BTTB** by **BTHTHB**

[7] N. K. Bose and P. Liang, "Neural Network Fundamentals with Graphs, Algorithms, and Applications," *McGraw Hill*, New York, 1996 .